by nucleosomes, strongly suggests that RCC1 binds H2A/H2B on chromatin, possibly at surfaces exposed on the faces of each nucleosome.

References and Notes

1. M. Hetzer, D. Bilbao-Cortes, T. C. Walther, O. J. Gruss, I. W. Mattaj, *Mol. Cell* **5**, 1013 (2000).
2. C. Zhang, P. R. Clarke, *Science* **288**, 1429 (2000).
3. M. Dasso, *Cell* **104**, 321 (2001).
4. D. Görlich, U. Kutay, *Annu. Rev. Cell Dev. Biol.* **15**, 607 (1999).
5. H. Seino, N. Hisamoto, S. Uzawa, T. Sekiguchi, T. Nishimoto, *J. Cell Sci.* **102**, 393 (1992).
6. C. A. Mizzen, J. E. Brownell, R. G. Cook, C. D. Allis, *Methods Enzymol.* **304**, 675 (1999).
7. Recombinant proteins were prepared as described (*22*). Equal amounts of each GST-fusion protein were bound to glutathione-Sepharose (Pharmacia) then blocked in 5% bovine serum albumin/phosphate-buffered saline (w/v). Assays were carried out {in 20 mM 3-[*N*-morpholino]propanesulfonate, pH 7.1, 100 mM potassium acetate, 5 mM magnesium acetate, 1 mM dithiothreitol, and 0.05% Tween-20 (v/v)} for 60 min at 4°C with intact nucleosomes (*6*), trypsinized nucleosomes (*23*), purified chicken histones, or isolated H2A or H2B (Roche) (all 1 μM or the indicated concentration). Where indicated, Ran, Ran(T24N), or Ran(Q69L) were added (10 μM). Free histones were isolated on SP-Sephadex beads (Pharmacia). After washing both sets of beads, the proteins were eluted, subjected to SDS–polyacrylamide gel electrophoresis (SDS-PAGE), and stained with Coomassie.
8. P. Cheung, C. D. Allis, P. Sassone-Corsi, *Cell* **103**, 263 (2000).
9. M. E. Nemergut, I. G. Macara, unpublished data.
10. V. Karantza, E. Freire, E. N. Moudrianakis, *Biochemistry* **35**, 2037 (1996).
11. F. R. Bischoff, C. Klebe, J. Kretschmer, A. Wittinghofer, H. Ponstingl, *Proc. Natl. Acad. Sci. U.S.A.* **91**, 2587 (1994).
12. C. Klebe, F. R. Bischoff, H. Ponstingl, A. Wittinghofer, *Biochemistry* **34**, 639 (1995).
13. S. A. Richards, K. M. Lounsbury, I. G. Macara, *J. Biol. Chem.* **270**, 14405 (1995).
14. Supplementary material is available on *Science* Online at www.sciencemag.org/cgi/content/full/292/5521/1540/DC1.
15. A. W. Murray, *Methods Cell Biol.* **36**, 581 (1991).
16. A. Philpott, G. H. Leno, R. A. Laskey, *Cell* **65**, 569 (1991).
17. A. Philpott, G. H. Leno, *Cell* **69**, 759 (1992).
18. M. Dasso, H. Nishitani, S. Kornbluth, T. Nishimoto, J. W. Newport, *Mol. Cell Biol.* **12**, 3337 (1992).
19. G. H. Leno, *Methods Cell Biol.* **53**, 497 (1998).
20. *Xenopus* sperm nuclei (10^5/ml) were incubated in a high-speed supernatant from a *Xenopus* egg lysate or in sperm buffer [20 mM Hepes (pH 7.7), 100 mM KCl, and 1 mM $MgCl_2$] for 10 min (*15*). After washing, chromatin-bound proteins were eluted, subjected to SDS-PAGE, and immunoblotted with anti–*Xenopus*-RCC1 serum. Alternatively, RCC1-GFP (500 nM) was added to the above reactions. Samples were treated with formaldehyde and 4′,6′-diamidino-2-phenylindole (DAPI) and analyzed immediately by fluorescence microscopy.
21. *Xenopus* sperm nuclei (10^5/ml) were incubated in sperm buffer with or without NplC (1 mg/ml) for 10 min at 25°C. The indicated GFP fusion protein (500 nM) was added with or without human histones (1 mg/ml) for 10 min at 25°C. Samples were fixed, stained, and analyzed (*20*). Where indicated, the GFP-fusion proteins were omitted and the nuclei were subjected to a two-dimensional gel analysis (*17*).
22. M. E. Nemergut, I. G. Macara, *J. Cell Biol.* **149**, 835 (2000).
23. A. E. de la Barre *et al.*, *EMBO J.* **19**, 379 (2000).
24. C. Klebe, H. Prinz, A. Wittinghofer, R. S. Goody, *Biochemistry* **34**, 12543 (1995).

25. We thank M. Dasso for providing the anti–*Xenopus*-RCC1 serum, D. Görlich for the NplC and BIB expression vectors, and T. Nishimoto for the RCC1 cDNA. Supported by grant GM-50526 from NIH, Department of Health and Human Services.

21 February 2001; accepted 10 April 2001

REPORTS

Protective Role of ATP-Sensitive Potassium Channels in Hypoxia-Induced Generalized Seizure

Katsuya Yamada,[1]* Juan Juan Ji,[1]* Hongjie Yuan,[1] Takashi Miki,[4] Shinichi Sato,[1] Naoki Horimoto,[1] Tetsuo Shimizu,[2] Susumu Seino,[4] Nobuya Inagaki[1,3]†

Adenosine triphosphate (ATP)–sensitive potassium (K_{ATP}) channels are activated by various metabolic stresses, including hypoxia. The substantia nigra pars reticulata (SNr), the area with the highest expression of K_{ATP} channels in the brain, plays a pivotal role in the control of seizures. Mutant mice lacking the Kir6.2 subunit of K_{ATP} channels [knockout (KO) mice] were susceptible to generalized seizures after brief hypoxia. In normal mice, SNr neuron activity was inactivated during hypoxia by the opening of the postsynaptic K_{ATP} channels, whereas in KO mice, the activity of these neurons was enhanced. K_{ATP} channels exert a depressant effect on SNr neuronal activity during hypoxia and may be involved in the nigral protection mechanism against generalized seizures.

K_{ATP} channels (*1*) couple the intracellular metabolic state to electrical activity at the plasma membrane (*2*). We have previously reported the molecular structure of K_{ATP} channels (*3*, *4*) comprising the inwardly rectifying K^+ channel Kir6.2 and a sulfonylurea receptor with high affinity (SUR1 in pancreatic β cells) or low affinity (SUR2A in the heart) for sulfonylureas. High-affinity binding of [^{3}H]glibenclamide in the brain is strongest in the SNr, suggesting high expression of the β cell type K_{ATP} channel in this nucleus (*5*, *6*). Because the SNr acts as a central gating system in the propagation of seizure (*7*–*9*) and generalized seizures can be evoked by metabolic stresses such as hypoxia and hypoglycemia (*10*), these K_{ATP} channels could well be involved in the development of seizure during ATP-depleted conditions.

Kir6.2 KO mice (*11*) were used to evaluate this possibility. Daily behavior and basal physiological values of KO mice were not significantly different from those of wild-type mice (*12*, *13*). However, responses to brief (150 s) hypoxia caused by oxygen deprivation ($n = 19$, 5.4 ± 0.2% O_2) differed in KO and wild-type mice (*14*). The wild-type mice (10/10) all remained sedated during the challenge and revived normally. In contrast, the KO mice all responded with a myoclonic jerk (latency = 8.9 ± 1.1 s, $n = 9$) followed by severe tonic-chronic convulsion and death (survival time = 21.8 ± 5.2 s, $n = 9$) (Table 1). Under more severe hypoxic conditions ($n = 6$, 4.3 ± 0.2% O_2, $P < 0.0001$ compared with 5.4 ± 0.2% O_2), four of the six wild-type mice exhibited a generalized convulsion (latency = 25.8 ± 2.7 s) (*15*). Electroencephalogram (EEG) and electromyogram (EMG) (*14*) revealed a sequence of seizure patterns in conscious KO mice ($n = 5$) challenged with 5.4 ± 0.1% O_2 (Fig. 1A). First, very low-voltage EEG for about 3 s indicated loss of consciousness. Then fast waves after an abrupt, sharp deflection lasted for several seconds in the EMG traces, corresponding to the tonic convulsion and myoclonus, after which bilateral, high-voltage sharp wave bursts were observed in the EEG traces. In wild-type mice under the same conditions, a medium- to low-voltage EEG predominated during the hypoxic period (Fig. 1B). This suggests that K_{ATP} channels participate in determining the seizure threshold during hypoxia. It is unlikely that the seizures observed in KO mice were produced by rapid cardiac arrest, because heartbeats continued after the seizure (*16*).

To investigate the role of SNr neuron activity, we recorded single unit activities from the SNr in acute slice preparations (*17*). In control, the firing rate of SNr neurons was not significantly different in wild-type and KO mice [25.2 ± 1.8 Hz ($n = 60$) and 22.6 ± 2.1 Hz ($n = 47$) for wild-type and KO mice, respectively]. However, in brief hypoxia (90 s) (*18*), wild-type neurons showed a marked decrease in firing rate to about one-third that before hypoxia (from 28.4 ± 2.0 Hz to 10.2 ± 3.2 Hz, $n = 9$, $P = 0.0003$; Fig. 2, A

[1]Department of Physiology and [2]Department of Psychiatry, Akita University School of Medicine, and [3]CREST of Japan Science and Technology Cooperation (JST), 1-1-1, Hondo, Akita 010-8543, Japan. [4]Department of Cellular and Molecular Medicine, Graduate School of Medicine, Chiba University, 1-8-1 Inohana Chuo-Ku, Chiba 260-8670, Japan.

*These authors contributed equally to this work.
†To whom correspondence should be addressed: E-mail: inagaki@med.akita-u.ac.jp

and C), whereas the firing rate of the KO neurons increased about 1.8-fold (from 30.6 ± 1.6 Hz to 53.8 ± 3.8 Hz, $n = 8$, $P = 0.0002$; Fig. 2, B and C). These results suggest that the K_{ATP} channel–mediated suppressive effect on SNr activity is sufficient to reverse the facilitation during hypoxia in these conditions.

To investigate the ionic mechanism of the suppression of SNr activity, we recorded from acutely dissociated neurons. γ-Aminobutyric acid–ergic (GABAergic) neurons, which constitute the majority of SNr neurons (*19*), were identified by their membrane electrical properties (*20*). With inside-out patch recordings, K_{ATP} channel currents were characterized in the SNr GABAergic neurons of wild-type mice (*21*). ATP decreased the open-state probability of the channels in a dose-dependent manner (half-maximal concentration = 12.0 μM, $n = 4$ to 8). It also was decreased significantly by tolbutamide (0.5 mM in the presence of 1 μM ATP) ($n = 11$, $P < 0.005$) and increased by the selective β cell K_{ATP} channel opener diazoxide (0.5 mM in the presence of 100 μM ATP) ($n = 7$, $P < 0.005$). The current-voltage relation showed inward rectification (conductance = 77.4 ± 0.3 pS; 140 mM K^+ on both sides of the membrane, $n = 7$; 1 μM ATP). No such channels were observed in the neurons of KO mice ($n = 32$). These results indicate that pancreatic β cell type K_{ATP} channels are functionally expressed in the SNr neurons of wild-type mice but not in KO mice. This confirms cell-attached patch (*22*) and reverse transcriptase polymerase chain reaction experiments showing that SUR1 and Kir6.2 are expressed in SNr neurons, whereas no SUR2A, SUR2B, or Kir6.1 is expressed (*23*).

The responses to hypoxia of the SNr neurons and the involvement of the K_{ATP} channels were further investigated by perforated patches (*24*). Under control normoxic condition (oxygenated with 100% O_2), SNr neurons of both wild-type and KO mice exhibited similar tonic, high-frequency, spontaneous firings [10.8 ± 1.1 Hz ($n = 38$) and 13.0 ± 1.4 Hz ($n = 26$), respectively], and there was no significant difference in membrane properties (*20*). However, the membrane potentials of the SNr neurons were shifted in the opposite direction when these neurons were perfused with hypoxic solution (*25*). Wild-type SNr neurons were hyperpolarized, and the hyperpolarization was reversed by tolbutamide (0.1 mM, $n = 10$) (Fig. 3A). Diazoxide (0.3 mM) also produced hyperpolarization of −5.6 ± 0.8 mV ($P < 0.0001$, $n = 22$) (Fig. 3A). In contrast, KO neurons showed no such hyperpolarization but were depolarized (Fig. 3B). During the 20-min perfusion with hypoxic solution, wild-type and KO SNr neurons elicited the maximal hyperpolarization of −9.6 ± 1.0 mV ($P < 0.0001$, $n = 13$) and maximal depolarization of 7.9 ± 1.0 mV ($P < 0.0001$, $n = 15$), respectively (Fig. 3C). The hyperpolarizing effect of hypoxia on wild-type SNr neurons was mimicked by the mitochondrial metabolic inhibitor 2,4-dinitrophenol (30 μM) (*16*).

The contribution of postsynaptic K_{ATP} channels to the response to hypoxia of the GABAergic SNr neurons also was examined in acute slice preparations. When both excitatory and inhibitory fast neurotransmissions were blocked by a combination of 6-cyano-7-nitroquinoxaline-2,3-dione (CNQX) (20 μM), D,L-2-amino-5-phosphonovaleric acid (DL-APV) (50 μM), and bicuculline (20 μM), the firing rate of both wild-type and KO SNr neurons increased about 35% during the normoxic condition (36.4 ± 6.3%, $n = 7$, $P = 0.0009$ and 33.7 ± 4.4%, $n = 6$, $P = 0.0011$, respectively) (Fig. 4, A and B). However, hypoxia produced striking contrasts in the firing of wild-type and KO neurons (Fig. 4, A, B, and C). In addition, tolbutamide (200 μM) reversed the hypoxia-induced decrease in the firings of wild-type neurons. This in-

Table 1. KO mice are susceptible to seizure by hypoxia. The mice were subjected to brief (150 s) hypoxia. Inspired oxygen concentrations are indicated. The ambient temperature was 23.0° to 25.6°C. Values are expressed as means ± SD. *, $P < 0.0001$ versus 5.4 ± 0.2 (unpaired t test).

	Oxygen concentration (%)			
	5.4 ± 0.2		7.3 ± 0.3*	
Mouse type	Wild type	KO	Wild type	KO
Number of mice	10	9	11	11
Number of mice that exhibited generalized convulsion	0	9	0	2
Convulsion onset (s)	–	8.9 ± 1.1	–	14.5 ± 2.1
Number of mice revived	10	0	11	11
Onset of cessation of respiration (s)	–	21.8 ± 5.2	–	–

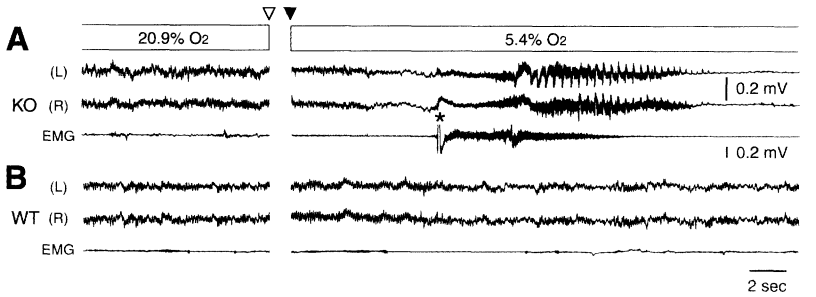

Fig. 1. A generalized convulsive seizure in KO mice. (**A**) Representative EEG and neck-muscle EMG traces in a KO mouse just before application of N_2 (in normoxia, 20.9% O_2, horizontal bar) and for the initial 27 s of hypoxia (5.4% O_2, total duration = 150 s). The myoclonus (asterisk) followed by the bilateral, convulsive seizure is represented. L and R, EEG traces from left and right cortices. Open and solid triangles, the onset and end of N_2 flow delivery, respectively. (**B**) Data from a wild-type (WT) mouse.

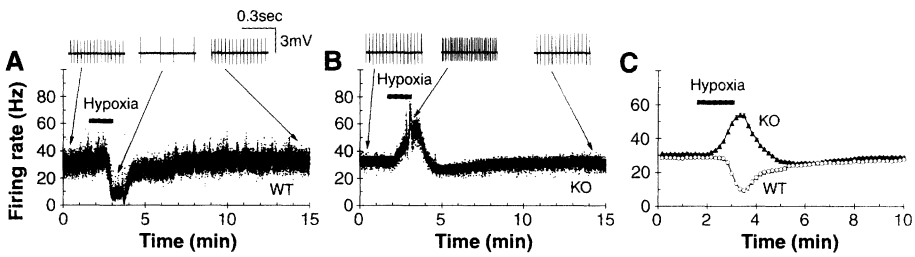

Fig. 2. Effect of hypoxia on firing rate of SNr neurons in acute slice preparations. Brief (90 s) hypoxia (solid bar) produced a marked decrease in firing rate of SNr neuron of wild-type mouse (**A**) but increased it in KO mouse (**B**). Insets represent traces of unit activities before, during, and after hypoxia (arrows). Spike amplitude increased in wild-type but decreased in KO mouse during hypoxia. (**C**) Hypoxia-induced changes in firing rate of wild-type (open circles, $n = 9$ from nine mice) and KO (solid triangles, $n = 8$ from eight mice) mice. Data points represent means ± SE.

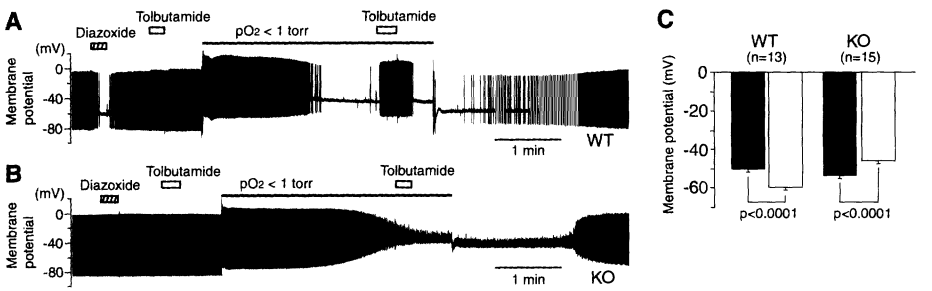

Fig. 3. Hypoxia produced contrary effects on membrane potential of wild-type and KO SNr neurons. (**A**) Acutely dissociated wild-type SNr neuron is hyperpolarized with cessation of firings by diazoxide (0.3 mM, hatched bar) and by hypoxia (pO_2 < 1 torr, solid line). Tolbutamide (0.1 mM, open bar) had no effect at resting potential but reversed hypoxia-induced hyperpolarization. (**B**) KO SNr neurons were depolarized during hypoxia. Both diazoxide and tolbutamide had no effect on membrane potential. The thick baseline at the end of the hypoxic period consists of spikes of very low amplitude. Recordings were performed by nystatin patch in the current clamp mode. The membrane potential gap observed at the onset and end of hypoxia is an artifact of solution switching. (**C**) Effect of hypoxia on membrane potentials of wild-type (n = 13) and KO (n = 15) mice. Solid and open columns represent membrane potentials in the normoxic condition and maximal hypoxic response, respectively. Values are means ± SE.

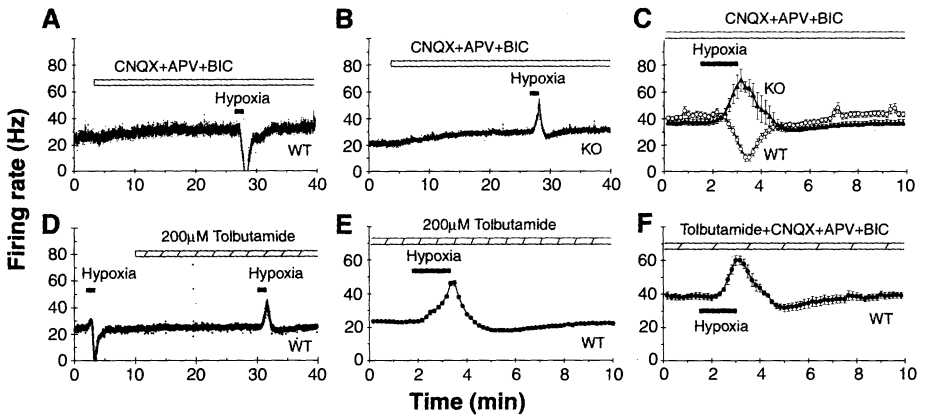

Fig. 4. Effect of synaptic transmission blockade and tolbutamide on hypoxia-induced change in firing rate of SNr neurons. The combination of 20 μM CNQX, 50 μM DL-APV (APV), and 20 μM bicuculline (BIC) had no effect on hypoxia-induced change in firing rate of wild-type (**A**) and KO (**B**) neurons, although it increased the firing rate in the normoxic condition in both groups. (**C**) Changes in firing rate of wild-type (open circles, n = 4 from four mice) and KO (solid triangles, n = 3 from three mice) mice due to hypoxia in the presence of three blockers. (**D**) Tolbutamide (200 μM) reversed the decrease in firing rate because of hypoxia to an increase in a wild-type neuron. (**E**) Changes in firing rate of wild-type neurons (solid circles, n = 6 from six mice) due to hypoxia in the presence of 200 μM tolbutamide. (**F**) As in (E), but with blockers to neurotransmissions added (solid circles, n = 6 from six mice). The data points show means ± SE in (C), (E), and (F).

crease was seen in the absence (P = 0.0042, n = 6; Fig. 4, D and E) or presence (P = 0.018, n = 4; Fig. 4F) of CNQX, APV, and bicuculline. Tolbutamide had no effect on firings in normoxia (n = 8, Fig. 4D). These results suggest that postsynaptic K_{ATP} channels are critical in the hypoxia-induced inactivation of the SNr neurons seen in wild-type mice, although presynaptic modulatory effects on firings have been described (*26*, *27*).

The cellular mechanisms that produce spike facilitation and membrane depolarization in KO SNr neurons are not clear. Inactivation of Na^+-K^+ adenosine triphosphatase or participation of other types of ATP-dependent and/or O_2-sensitive pathways may be possible (*28*). However, activation of the K_{ATP} channels reversed this facilitatory effect in wild-type mice, showing the crucial role of the K_{ATP} channels during hypoxia.

We propose that inactivation of SNr neurons after opening of K_{ATP} channels protects against seizure propagation during metabolic stress. Extracellular field potentials in cerebral cortex slices evoked by electrical stimulation of the underlying white matter were not altered during hypoxic conditions (90 s) either in KO or wild-type mice (*16*). A similar result was reported in hippocampus (*29*). This suggests that SNr neurons, being extremely sensitive to hypoxia, may act as a sensor for hypoxic conditions, although the possibility that other brain regions also are involved cannot be excluded (*30*). The SNr has been proposed as a key site of the activity of anticonvulsant drugs that enhance GABA-mediated inhibition of seizures (*7*, *31*), and blockade of excitatory neurotransmission in the nucleus raises the threshold for seizures (*8*). The present study, therefore, suggests the therapeutic potential of selective agonists to this specific K_{ATP} channel in the treatment of brain disorders associated with ATP insufficiency such as stroke and metabolic encephalopathies.

References and Notes

1. A. Noma, *Nature* **305**, 147 (1983).
2. F. M. Ashcroft, *Annu. Rev. Neurosci.* **11**, 97 (1988).
3. N. Inagaki *et al.*, *Science* **270**, 1166 (1995).
4. S. Seino, *Annu. Rev. Physiol.* **61**, 337 (1999).
5. C. Mourre, Y. Ben Ari, H. Bernardi, M. Fosset, M. Lazdunski, *Brain Res.* **486**, 159 (1989).
6. G. A. Hicks, A. L. Hudson, G. Henderson, *Neuroscience* **61**, 285 (1994).
7. M. J. Iadarola, K. Gale, *Science* **218**, 1237 (1982).
8. G. De Sarro, B. S. Meldrum, C. Reavill, *Eur. J. Pharmacol.* **106**, 175 (1985).
9. A. Depaulis, M. Vergnes, C. Marescaux, *Prog. Neurobiol.* **42**, 33 (1994).
10. B. J. Fisch, *Fisch and Spehlmann's EEG Primer* (Elsevier, Amsterdam, ed. 3, 1999), pp. 301–303.
11. T. Miki *et al.*, *Proc. Natl. Acad. Sci. U.S.A.* **95**, 10402 (1998).
12. Male BL6 unaffected (Kir6.2$^{+/+}$; wild type) and homozygous (Kir6.2$^{-/-}$; KO) mice were used according to the protocols reviewed and approved by the Akita University Institutional Committee for Animal Studies. Physiological values including body weight, rectal temperature, blood gas, pH, heart rate, blood pressure, respiratory rate, and O_2 consumption of KO mice were not significantly different from wild-type mice (see Web tables 1 to 4) (*13*).
13. See supplementary material on *Science* Online at www.sciencemag.org/cgi/content/full/292/5521/1543/DC1.
14. Unanesthetized 8- to 13-week-old male mice were used. A rapid decrease in the ambient inspired fraction of O_2 was obtained within 8 s. See supplementary material (*13*) for details of the methods used in the hypoxia experiment in vivo.
15. To evaluate statistical significance, we subjected data to analysis of variance and Bonferroni/Dunn test or Student's t test.
16. K. Yamada, J.-J. Ji, N. Inagaki, unpublished data.
17. The brain cytoarchitecture of wild-type and KO mice appeared to be similar (see Web fig. 1) (*13*). A 500-μm-thick, quasi-coronal slice containing the SNr was dissected from 9- to 11-week-old male mice. The slice was placed on an interface-type recording chamber at 33°C and superfused (0.6 ml/min) with Krebs-Ringer solution [127 mM NaCl, 2 mM KCl, 2.4 mM $CaCl_2$, 1.3 mM $MgSO_4$, 1.24 mM KH_2PO_4, 26 mM $NaHCO_3$, and 10 mM glucose (pH 7.4)] saturated with 95% O_2/5% CO_2 [referred to as normoxic condition; pO_2, about 680 mm of Hg measured by a gas analyzer (1H26)]. Extracellular unit recordings were obtained at 50 to 430 μm in depth, and no statistical difference in spike half-width (0.17 to 0.32 ms) and firing rate (2.2 to 62 Hz) was observed between wild-type and KO mice.
18. A brief hypoxia was induced by superfusing the slice with a solution equilibrated with 95% air/5% CO_2 instead of 95% O_2/5% CO_2. pO_2 fell to about 215 torr in the gas phase within the chamber at 90 s after onset of the hypoxic superfusion. For comparison of firing rates, we selected neurons 145 to 165 μm in depth that exhibited firing rates at 20 to 40 Hz in the normoxic solution. pO_2 values 150 μm in depth were assumed to be below 20 torr (*32*). Hypoxic solutions reached the slice no later than 12 s after turning an electromagnetic valve. Drugs were applied to the bath.
19. W. H. Oertel, M. L. Tappaz, A. Berod, E. Mugnaini, *Brain Res. Bull.* **9**, 463 (1982).
20. Single neurons were dissociated from the rostral half

of the SNr of 15- to 20-day-old mice by papain digestion. Spontaneously firing (>3Hz), medium-sized (15 to 25 μm) neurons, the major constituent of SNr cells, which had no hyperpolarization-activated current (I_h) in perforated whole-cell patch recordings (*24*), were analyzed. Membrane properties were similar to those reported for SNr GABAergic neurons (*27*, *33*, *34*) (see Web fig. 2) (*13*). This was verified by immunostaining with antibodies to glutamic acid decarboxylase in separate experiments. GABAergic SNr neurons of wild-type and KO mice had similar resting membrane potentials of −52.3 ± 0.9 mV (n = 38) and −51.4 ± 1.2 mV (n = 26), respectively, and membrane input resistance was 2.3 ± 0.2 gigaohms (n = 33) and 2.4 ± 0.3 gigaohms (n = 23), respectively.

21. See Web fig. 3 (*13*) for details of single-channel analyses.
22. C. Schwanstecher, U. Panten, *Naunyn-Schmiedeberg's Arch. Pharmacol.* **348**, 113 (1993).
23. B. Liss, R. Bruns, J. Roeper, *EMBO J.* **18**, 833 (1999).
24. For nystatin-perforated patch recordings, the patch pipettes (2 to 4 megaohms) contained 150 mM KCl, 10 mM Hepes, and nystatin (50 μg/ml; pH 7.2). The standard bath solution [150 mM NaCl, 5 mM KCl, 1 mM $MgCl_2$, 2 mM $CaCl_2$, 10 mM Hepes, and 10 mM glucose (pH 7.4)] was oxygenated with 100% O_2 and perfused (10 ml/min) at 22° to 24°C. The pipette access resistance was compensated.
25. Hypoxia was introduced by exchanging the perfusion medium from that equilibrated with 100% O_2 to a solution containing 2 mM $Na_2S_2O_4$ bubbled with 100% N_2 (<1 torr, measured with a gas analyzer).
26. S. Amoroso, H. Schmid-Antomarchi, M. Fosset, M. Lazdunski, *Science* **247**, 852 (1990).
27. I. M. Stanford, M. G. Lacey, *Neuroscience* **74**, 499 (1996).
28. L. L. Dugan, D. W. Choi, in *Basic Neurochemistry*, G. J. Siegel *et al.*, Eds. (Lippincott-Raven, Philadelphia, ed. 6, 1999), pp. 711–729.
29. A. J. Hansen, J. Hounsgaard, H. Jahnsen, *Acta Physiol. Scand.* **115**, 301 (1982).
30. I. Lamensdorf, N. Meiri, J. Harvey-White, D. M. Jacobowitz, I. J. Kopin, *Brain Res.* **818**, 275 (1999).
31. L. Turski *et al.*, *Brain Res.* **520**, 232 (1990).
32. C. Jiang, S. Agulian, G. G. Haddad, *Brain Res.* **568**, 159 (1991).
33. C. D. Richards, T. Shiroyama, S. T. Kitai, *Neuroscience* **80**, 545 (1997).
34. C.-W. Wu, C. K. S. Leung, W.-H. Yung, *Neuroreport* **7**, 2513 (1996).
35. Supported by Scientific Research Grants, a Grant-in-Aid for Scientific Research on Priority Areas "ABC Proteins" (grant 10217201), and Creative Basic Research (10NP0201) from the Ministry of Education, Culture, Sports, Science and Technology of Japan. We thank M. Nakata, T. Furukawa, H. Takahashi, K. Kato, Y. Hanaoka, and K. Shibata for technical assistance and M. Lazdunski for critical reading of the manuscript.

13 February 2001; accepted 19 April 2001

Requirement of DNase II for Definitive Erythropoiesis in the Mouse Fetal Liver

Kohki Kawane,[1]* Hidehiro Fukuyama,[1]* Gen Kondoh,[2] Junji Takeda,[2] Yoshiyuki Ohsawa,[3] Yasuo Uchiyama,[3] Shigekazu Nagata[1]†

Mature erythrocytes in mammals have no nuclei, although they differentiate from nucleated precursor cells. The mechanism by which enucleation occurs is not well understood. Here we show that deoxyribonuclease II (DNase II) is indispensable for definitive erythropoiesis in mouse fetal liver. No live DNase II–null mice were born, owing to severe anemia. When mutant fetal liver cells were transferred into lethally irradiated wild-type mice, mature red blood cells were generated from the mutant cells, suggesting that DNase II functions in a non–cell-autonomous manner. Histochemical analyses indicated that the critical cellular sources of DNase II are macrophages present at the site of definitive erythropoiesis in the fetal liver. Thus, DNase II in macrophages appears to be responsible for destroying the nuclear DNA expelled from erythroid precursor cells.

Apoptosis is usually accompanied by DNA degradation that is regulated by caspase-activated DNase (CAD) (*1*). We recently showed that apoptotic DNA fragmentation occurs in macrophages in the absence of CAD after the apoptotic cells are phagocytosed (*2*), suggesting that DNase II, a lysosomal DNase (*3*, *4*), degrades DNA of apoptotic cells. Nuc-1, which is responsible for the apoptotic DNA fragmentation in *Caenorhabditis elegans*, has recently been identified as a homolog of DNase II (*5*). To investigate the physiological roles of DNase II in mammals, we generated mice deficient in the enzyme.

The murine DNase II gene is encoded by six exons within 2.3 kb of genomic DNA (*6*). We constructed a targeting vector, in which exons 1 to 5 and part of exon 6 were replaced with the *neo* gene (Fig. 1A) (*7*). The vector was introduced into R1 mouse embryonic stem (ES) cells, and G-418–resistant transformants containing the mutation in one allele of the DNase II gene were established (Fig. 1B). The ES clones were aggregated with eight-cell embryos, and the embryos were implanted into foster mothers. Chimeric mice derived from four clones transmitted the mutation to their offspring (F_1). The DNase $II^{+/-}$ mice were healthy and fertile. However, no live DNase $II^{-/-}$ mice were found among the progeny (F_2) of the DNase $II^{+/-}$ intercrosses. Analysis of timed pregnancies revealed that DNase $II^{-/-}$ embryos, confirmed by Southern hybridization (Fig. 1C), were present at a frequency roughly consistent with Mendelian inheritance throughout the embryonal stages (*8*).

Northern hybridization analysis indicated that the DNase II gene was expressed in the fetal liver of the wild-type and DNase $II^{+/-}$ embryos, but not in the DNase $II^{-/-}$ liver (Fig. 2A). The gene encoding erythroid Krüppel-like factor (EKLF), a transcription factor that is indispensable for erythroid cell differentiation (*9*, *10*), is located 3.9 kb upstream of the DNase II gene (*6*) (Fig. 1A). EKLF and β^{major}-globin mRNAs at embryonic day 14.5 (E14.5) were expressed in the fetal liver of DNase $II^{-/-}$ embryos at levels similar to those in normal fetal liver (Fig. 2A), indicating that the expression and function of EKLF were not impaired in DNase $II^{-/-}$ embryos. Other DNases such as DLAD and Xib have properties (acidic pH optimum and no requirement for divalent cations) similar to those of DNase II (*11*, *12*). To examine whether these enzymes compensated for loss of DNase II, we assayed extracts from E14.5 fetal livers for DNase activity (*13*). As shown in Fig. 2B, cell extracts from normal or heterozygous fetal liver showed substantial DNase activity at pH 5.7, whereas little, if any, DNase activity was detected under these conditions in the extracts from DNase $II^{-/-}$ fetal liver. In contrast, the DNase I–like activity determined at neutral pH in the presence of Ca^{2+} and Mg^{2+} was normal or slightly higher in the extracts from DNase $II^{-/-}$ fetal liver.

Homozygous DNase $II^{-/-}$ embryos were apparently normal until E12.5, when a normal level of vasculature was seen in the embryos and yolk sac (Fig. 3A). Histological studies revealed similar numbers of nucleated primitive erythrocytes in the peripheral blood of normal and DNase $II^{-/-}$ embryos at E12.5 (*14*). However, some DNase $II^{-/-}$ embryos became paler than the wild-type embryo at E14.5, and all mutant embryos were severely anemic by E17.5 (Fig. 3B). The number of mature erythrocytes in the peripheral blood of

[1]Department of Genetics, Osaka University Medical School, and Core Research for Evolutional Science and Technology, Japan Science and Technology Corporation, Suita, Osaka 565-0871, Japan. [2]Department of Social and Environmental Medicine, Osaka University Medical School, Suita, Osaka 565-0871, Japan. [3]Department of Cell Biology and Anatomy, Osaka University Medical School, Suita, Osaka 565-0871, Japan.

*These authors contributed equally to this work.
†To whom correspondence should be addressed. E-mail: nagata@genetic.med.osaka-u.ac.jp